Reuse of shale gas flowback and produced water: Effects of coagulation and adsorption on ultrafiltration, reverse osmosis combined process

Reuse of shale gas flowback and produced water: effects of coagulation and adsorption on ultrafiltration, reverse osmosis combined process

Revised for

Science of the Total Environment

Wei Shang [a], Alberto Tiraferri [b], Qiping He [c], Naiwen Li [d], Haiqing Chang [a], Chao Liu [d], and Baicang Liu [a, *]

[a] College of Architecture and Environment, Institute of New Energy and Low-Carbon Technology, Institute for Disaster Management and Reconstruction, Sichuan University, Chengdu, Sichuan 610207, PR China

[b] Department of Environment, Land and Infrastructure Engineering, Politecnico di Torino, Corso Duca degli Abruzzi 24, 10129 Turin, Italy

[c] Chuanqing Drilling Engineering Company Limited, Chinese National Petroleum Corporation, Chengdu 610081, PR China

[d] College of Water Resource & Hydropower, State Key Laboratory of Hydraulics and Mountain River Engineering, Sichuan University, Chengdu, Sichuan 610065, PR China

* Corresponding author: Baicang Liu, Email: bcliu@scu.edu.cn

Abstract

The shale gas flowback and produced water (FPW) from hydraulic fracturing in the Sichuan province of China has relatively low to moderate levels of total dissolved solids (< 20 g/L) and organics (< 50 mg/L of dissolved organic carbon). As such, a combined ultrafiltration (UF), reverse osmosis (RO) system can be successfully applied to desalinate this feed water with the goal of reuse. However, the concentration of influent organic matter and particulates in the UF and RO stage is high, and the overall ionic and organics composition is highly complex, so that the membrane processes do not perform well, also due to fouling. To ensure the long-term and efficient operation of the UF-RO stages, a combined pretreatment of the FPW with coagulation and adsorption was investigated. The effect of different parameters on the performance on the system was studied in detail. Overall, the coagulation-adsorption pre-treatment greatly reduced fouling of the membrane processes, thanks to the high removal rate of turbidity (98.8%) and dissolved organic carbon (80.4%). The adsorption of organic matter by powdered activated carbon was best described by the Freundlich equilibrium model, with a pseudo second-order model representing the adsorption kinetics. Also, the various ions had competitive removal rates during the adsorption step, a phenomenon reported for the first time for FPW treatment. Also, an optimal dose of activated carbon existed to maximize fouling reduction and effluent quality. The overall treatment system produced a high-quality water streams, suitable for reuse.

Keywords: Flowback and produced water, Adsorption, Coagulation, Ultrafiltration, Reverse osmosis, Water quality

1. Introduction

Shale gas has attracted attention in the energy field as an unconventional natural gas resource with potentially low carbon footprint and globally abundant reserves (Butkovskyi et al., 2017; Estrada and Bhamidimarri, 2016; Howarth et al., 2011; Vidic et al., 2013). China has the world's largest shale gas reserves of 25.08 trillion cubic meters. The Sichuan Basin is China's largest storage of shale gas and includes the most productive commercial shale gas field (Zhang et al., 2019; Zou et al., 2018). However, a large amount of flowback and produced water (FPW) is produced during the process of mining shale gas, ranging from 5,200 to more than 25,000 m^3 for each horizontal well (Chang et al., 2019a; Kondash and Vengosh, 2015; Zou et al., 2018).

The hydraulic fracturing wastewaters are highly variable in their composition, both spatially and temporally (Barbot et al., 2013; Chang et al., 2019a). The high concentrations of particulates, colloids, hardness, salinity, organic matter, and radioactivity (Luek and Gonsior, 2017; Vengosh et al., 2014; Xiong et al., 2016), require extensive and non-conventional FPW treatment for its possible reuse or direct discharge (Chang et al., 2017). Compared to the FPW typically generated in basins in the USA (Chang et al., 2019a), the FPW from Sichuan basin is not only estimated to contain a lower level of TDS (6906 – 28,900 mg/L) (Chang et al., 2019a; Chen et al., 2015; Guo et al., 2018; Huang et al., 2016), but it is also characterized by a lower amount of organic matter (total organic carbon (TOC) is approximately 78 mg/L) (Kong et al., 2017). There are other important differences for the FPW from different regions, such as the types and mixture of ions, organic matters, and the presence of radioactive materials. The FPW has the potential to contaminate groundwater, soil, and air, posing great risks to human and ecosystem health in the case of improper management (Annevelink et al., 2016; Howarth et al., 2011; Shaffer et al.,

2013; Stoll et al., 2015). Therefore, for the Sichuan basin, China's shale gas mining areas, and the world at large, it is extremely urgent to create a process to manage a plethora of FPWs having each their own specific characteristics.

External reuse is a promising wastewater management approach for shale gas FPW (Butkovskyi et al., 2017; Chang et al., 2019a; Guo et al., 2018; Harkness et al., 2015). China, as well as the rest of the world, still lacks efficient processing technologies and rational systems for reuse of these streams in irrigation or for recycling in additional fracking operations. Reliable research on FPW reclamation is arguably the primary task of shale gas exploration at this stage. Membrane-based processes are certainly promising techniques for FPW recycling due to their high efficiency and excellent permeate quality (Chang et al., 2019a; Estrada and Bhamidimarri, 2016; Shaffer et al., 2013), including microfiltration, ultrafiltration, nanofiltration, forward osmosis (FO), reverse osmosis (RO), or their combination. Among them, reverse osmosis is regarded as the most energy-saving and promising water desalination technology (Elimelech and Phillip, 2011). However, membrane fouling is still one of the critical difficulties in the implementation of membrane filtration processes (Chang et al., 2019a). Numerous studies have been conducted to control or reduce membrane fouling, including optimization of operational parameters and application of effective pretreatment (Amin Reyhania, 2015).

Coagulation is a relatively simple physical-chemical technique to treat FPW, reducing organics and thus alleviating membrane fouling. Rosenblum et al. confirmed that coagulation could remove 80% of total petroleum hydrocarbons and 90% of turbidity (Rosenblum et al., 2016). In a previous study, 33.6-62.0% and 33.6-42.6% of COD was removed by addition of aluminum sulfate or ferric chloride, respectively, and 64% and 84% of UF fouling was decreased by these coagulants under optimal dosage (Chang et al., 2019b). However, the use of coagulants

results in an increase in the concentration of aluminum or iron in the effluent water. Adsorption may be thus applied to further polish this stream before further treatment based on membranes. Activated carbon is an excellent adsorbent which remains widely used, mainly due to its high adsorption capacity, adsorption speed, good mechanical stability (Liu et al., 2012), although the effect of powdered activated carbon (PAC) on membrane fouling is still debated (Shao et al., 2017; Wang et al., 2016). Additionally, the PAC regeneration process and the post-treatment of the adsorbed substances may also increase the operational cost. When treating FPW, PAC achieved greater than 80% reductions of the total ion chromatogram, while dissolved organic carbon (DOC) removals were between 9.5 and 48.3% (Rosenblum et al., 2016). The combined process of coagulation and adsorption can greatly reduce the dissolved organics, turbidity, and ion concentrations (Rosenblum et al., 2016), while also reducing the consumption of activated carbon. However, little research has been performed on such combined process, and specifically on its role to optimize membrane filtration processes in the treatment of FPW.

The objective of this study is to evaluate the feasibility of a hybrid coagulation-adsorption-UF-RO system in assisting FPW reuse in Weiyuan shale gas operation. The performance of the system, the influence of coagulation and activated carbon on membrane performance and their effects in the removal of dissolved organics are systematically investigated. The results of this study allow the evaluation of coagulation-adsorption to alleviate membrane fouling and the applicability of this process for the treatment of FPW. Another objective of the study is to provide a better understanding of UF and RO fouling from FPW and discuss solutions that enable the use of membrane filtration in the recycling of wastewater produced during shale gas exploration.

2. Materials and methods

2.1 Shale gas FPW samples

The flowback and produced water sample utilized in this study was collected from a well site of the Weiyuan shale gas field located in the Sichuan province of China. The site includes 6 horizontal wells that were hydraulically fractured on a single pad using similar fracturing fluid. Wastewater from previously completed wells and fresh water were mixed and stored in a storage pool. The stock samples were packed at the pool into plastic cylindrical containers and then transported to the lab. Its characteristics are summarized in Table 1. The containers were sealed and stored in a dark place to minimize variation of their characteristics in time.

Table 1. Quality of the influent water and of the effluents from each treatment step of the hybrid system investigated in this study[a]

Constituent	FPW in Weiyuan	Coagulation	PAC [b] Adsorption	UF membrane permeate	RO membrane permeate
Turbidity (NTU)	187	15.8	2.1	0.08	0.07
UV_{254} (1/cm)	0.137	0.077	0.015	0.016	0.003
TDS (mg/L)	16320	15715	15930	15410	224
Conductivity (mS/cm)	26.79	26.29	26.20	25.85	0.52
DOC (mg/L)	38.03	13.61	5.21	5.19	1.71
SUVA (L $mg^{-1}m^{-1}$)	0.36	0.46	0.21	0.22	0.17
pH	7.48	6.93	7.31	7.51	6.65
Na^+ (mg/L)	6151	6065	5920	5931	105
Ca^{2+} (mg/L)	274.7	257.9	201.2	200.9	1.1
Mg^{2+} (mg/L)	36.5	34.8	26.5	26.4	-
K^+ (mg/L)	255.1	246.2	175.7	173.3	2.5
Sr^{2+} (mg/L)	66.3	57.3	28.9	28.4	-
Ba^{2+} (mg/L)	94.4	90.2	63.9	61.3	-
NH_4^+ (mg/L)	60.4	60.2	50.1	50.3	1.3
Cl^- (mg/L)	9412	9275	9158	9133	149
NO_2^- (mg/L)	35.7	31.0	28.5	28.5	1.3
F^- (mg/L)	12.6	11.5	9.4	9.3	0.2
Br^- (mg/L)	97.9	94.2	89.8	89.8	1.7
NO_3^- (mg/L)	161.9	151.9	139.9	138.8	1.2

[a] The data in the table is the average of three replicate experimental data.

[b] Adsorption experiment at optimal dose of 300 mg/L of WP260.

2.2 Chemicals and materials

Aluminum sulfate octadeca hydrate ($Al_2(SO_4)_3 \cdot 18H_2O$; Sigma Aldrich, analytical grade) was used as a coagulant. The reagents for chemical oxygen demand (COD) analysis were purchased from Lianhua Tech Co., Ltd. (Lanzhou, China). Concentrated sulfuric acid was obtained from Kelong Chemical (Chengdu, China). Three types of powdered activated carbon (WP260, PAC70X, DCL320) were purchased from Calgon Carbon Corporation (Moon Township, PA, USA). The detailed characteristics of the activated carbon samples are listed in Table 2. The size distributions of these adsorbents are shown in Fig. S2 of the Supporting Information.

Table 2. Characteristics of three different activated carbon products investigated in this study

Product name	Specific surface area (m^2/g)	Total pore volume (cm^3/g)	Avg pore diameter (nm)	Moisture wt%	Ash wt%	US mesh (<325) wt%	Iodine No. (mg/g)
WP260	1392	1.05	3.01	6	14	72	1023
PAC70X	882	0.44	1.99	5	15	84	732
DCL320	933	0.54	2.31	7	-	80	-

A polyvinylidene fluoride (PVDF) hollow fiber membrane (Litree Purifying Technology Co., Ltd., Haikou, China) was employed for the UF treatment. This membrane (pore size in the range of 11.3-28.8 nm) had a molecular weight cut-off (MWCO) of 100 kDa, and the outside diameter of the fiber was 1.8 mm. In each UF test, a single fiber with a length of 20 cm was used, and the effective surface area was 11.3 cm^2. The SW21 from Vontron Membrane Technology Co., Ltd.

(Guiyang, China) was selected as RO membrane. The effective area of each RO membrane coupon was 14.6 cm^2.

2.3 Analytical methods

The temperature and pH were measured using a mercury thermometer and a pH meter, respectively (PB-10, Sartorius Scientific Instruments Co., Ltd., Beijing, China). The turbidity was determined with a Hach TL2310 (Hach, Loveland, CO, USA) turbidimeter. An Ultrameter II 6PFC (Myron L, Carlsbad, California, USA) portable multi-function instrument was adopted to determine the TDS and conductivity. The fast digestion-spectrophotometric method was utilized to measure the COD using a 5B-1F(V8) fast digestion instrument (Lianhua Environmental Protection Technology Co., Ltd., Lanzhou, China). UV absorbance at 254 nm was measured by UV-Vis spectrophotometry (Orion AquaMate 8000, Thermo Fisher Scientific Inc., MA, USA). The dissolved organic carbon (DOC) content was measured using a TOC analyzer L series (Shimadzu, Kyoto, Japan). $SUVA_{254}$ (L/mg·m), an indicator of aromatic dissolved organic matter, was defined as UV_{254} absorbance divided by DOC concentration. The quantification of the concentrations of Cl^-, Br^-, F^-, NO_2^-, NO_3^-, Na^+, K^+, NH_4^+, Ca^{2+}, Mg^{2+}, Ba^{2+}, Sr^{2+} was performed using a Dionex ICS-1100 ion chromatographer (Thermo Fisher Scientific Inc., MA, USA). The techniques of scanning electron microscopy (SEM) and energy dispersive spectroscopy (EDS) (Regulus 8230, HITACHI, Tokyo, Japan) were used to investigate the morphology and elemental ratio of the membrane surface and fouling layers. Before SEM-EDS analysis, the membranes were coated with 2 nm of gold using a magnetron sputter (MSP-2S, IXRF Systems, USA). The Brunauer-Emmett-Teller (BET) specific surface areas and porosity were determined by means of nitrogen-sorption isotherms with a NOVA 2200e analyzer (Quantachrome, USA).

2.4 Experimental procedures

2.4.1 Treatment protocols

The overall design of the proposed system (Fig. S1) is as follows: coagulation, activated carbon adsorption, ultrafiltration, and finally reverse osmosis. Unless otherwise specified, the operational temperature was 293 ± 1 K for all the experiments. In the jar coagulation tests, aluminum sulfate was chosen as flocculant and the optimum dose was 600 mg/L according to our previous work.(Chang et al., 2019b) Experiments were conducted with the ZR4-6 jar-test equipment (Zhongrun Water Industry Technology Development Co., Ltd., Shenzhen, China). After adding the coagulant to a raw water sample, the experimental procedure consisted of two subsequent stages: a rapid mixing stage at 200 rpm for 1 min followed by slow mixing at 40 rpm for 20 min. The stirring was then stopped, and the mixture was allowed to settle for 30 min. Finally, the supernatant was removed from the beaker for analysis and subsequent experiments. For adsorption experiments, the three types of PAC were rinsed with ultrapure water to remove undesired surface compounds and dried at 377 K for 24 h. The raw water or the samples obtained from coagulation tests were treated by adsorption with the addition of PAC in the jar-test equipment mentioned above, while stirring at 80 rpm for different time intervals in the range 15-120 min. A series of PAC dosages (50, 150, 300, 800, and 1200 mg/L) were tested.

New UF and RO membranes were soaked in ultrapure water for at least 48 h and the water was replaced at least three times. A new membrane was used for each UF run and a filtration with ultrapure water for 1 h was performed to obtain a stable water flux. Then, multi-cycle UF tests with periodic hydraulic backwash were executed at a constant flux equal to 50 L $m^{-2}h^{-1}$ (LMH). The duration of each filtration and backwash step was 54 min and 3.5 min, respectively, for each cycle. The transmembrane pressure (TMP) was measured using a pressure sensor (Unik

187 5000, General Electric Company, USA) in constant flux mode, which was controlled
188 continuously with a pressure gauge (1379 Duragauge, Ashcroft Inc., USA) connected to the
189 peristaltic pump. The permeate solution tank rested on an electronic balance (Adventurer Pro
190 CAV8101, Shanghai, China) and weight changes were recorded over time to determine the
191 permeate flux.

192 The RO unit was operated using a dead-end stirred cell (HP 4750, Sterlitech Corp., Kent,
193 WA, USA). These tests were carried out at the constant transmembrane pressure of 5.5 MPa (55
194 bar). The solution in the filtration cell was kept under stirring at 200 rpm. The initial feed volume
195 in the RO cell was 300 mL and the filtration was continued until a recovery rate of 50% was
196 achieved (150 mL of permeate solution was collected).

197 ***2.4.2 Analyses and calculations***

198 Following adsorption, the DOC content of the supernatant solution was measured. The uptake of
199 adsorbate by PAC, q_e (mg DOC/g), was calculated according to the following
200 equation(Sontheimer et al., 1988):

201 $$q_e = \frac{V\left(C_0 - C_e\right)}{m} \quad (1)$$

202 where q_e is the equilibrium adsorbent-phase concentration of adsorbate (mg adsorbate/g
203 adsorbent), C_0 and C_e are the initial and equilibrium liquid phase concentrations of the organic
204 adsorbates (mg DOC/L), respectively, V is volume of the solution (L), and m is the weight of the
205 PAC (g) adsorbent. Freundlich, Langmuir, and Temkin isotherm models were assessed to
206 describe the mechanism of phase partitioning. The Freundlich isotherm model can be expressed
207 by Eq. (2):(Cheng et al., 2015)

$$q_e = K_F C_e^{\frac{1}{n}} \quad (2)$$

Eq. (2) can also be expressed in the linearized logarithmic form:

$$\log(q_e) = \log(K_F) + \frac{1}{n}\log(C_e) \quad (3)$$

where K_F is the Freundlich adsorption capacity parameter, and $1/n$ is the dimensionless Freundlich adsorption intensity parameter. The intercept and slope of the line in equation 3 enable the determination of the isotherm constants. Langmuir isotherm model is expressed as:(Manz et al., 2016)

$$q_e = \frac{Q_M K_L C_e}{1 + K_L C_e} \quad (4)$$

The linear equation of Eq. (4) is expressed as:

$$\frac{C_e}{q_e} = \frac{C_e}{Q_M} + \frac{1}{K_L Q_M} \quad (5)$$

where K_L is the Langmuir adsorption constant, and Q_M is the maximum adsorbent phase when the absorbent is saturated. The Temkin isotherm model contains a factor that explicitly takes into account the adsorbate-adsorbent interactions. This model assumes the following: (i) the heat of adsorption of all the molecules in the layer decreases linearly with coverage due to adsorbent-adsorbate interactions, and (ii) the adsorption is characterized by a uniform distribution of binding energies, up to a maximum binding energy(Angin, 2014). The Temkin isotherm model is presented in the following form:

$$q_e = B\ln(K_T \cdot C_e) \quad (6)$$

Eq. (6) can be written in the linear form:

$$q_e = B\ln(K_T) + B\ln(C_e) \tag{7}$$

where B is the Temkin constant related to gas constant, heat of sorption, and absolute temperature, K_T is the equilibrium binding constant (L/mg). The adsorption coefficients can be computed by plotting q_e values vs. $ln\ C_e$.

In order to describe the speed of the adsorption process, pseudo first-order and pseudo second-order kinetic models were selected to assess the experimental data. The models were expressed with the following equations:(Cheng et al., 2015)

$$\log(q_e - q_t) = \log q_e - \frac{k_1 t}{2.303} \tag{8}$$

$$\frac{t}{q_t} = \frac{1}{k_2 q_e^2} + \frac{t}{q_e} \tag{9}$$

where q_e and q_t (mg/g) are the adsorbent capacities at equilibrium and at time t (h), respectively; k_1 (h^{-1}) and k_2 (g/(mg·h)) are the pseudo first-order and pseudo second-order rate constants, respectively.

The total fouling index (TFI) was used to quantify the UF membrane fouling of different operational cycles and cleaning steps (Chang et al., 2016; Nguyen et al., 2011). The derivation process for the TFI parameter is provided in the SI. And the TFI was calculated by equation (10):

$$(TFI)V_s = \frac{TMP_f}{TMP_0} - 1 \tag{10}$$

where V_s (L/m^2) is the volume of filtered water per unit membrane area; the TMP at the beginning and end of the filtration is represented by TMP_0 and TMP_f (kPa), respectively. This index was calculated by the least square linear regression approach.

3. Results and discussion

3.1 Adsorption processes

3.1.1 Adsorption isotherms

Fig. 1A-B depicts the isotherms for the adsorption of DOC onto PAC70X, WP260, and DCL320 adsorbents. To evaluate the maximum adsorption capacities of three types of PAC toward DOC, the adsorption isotherms were obtained with the pH fixed at 7.5. The regression Freundlich, Langmuir, and Temkin constants are presented in Table 3. The Freundlich isotherm equation appears to be the most suitable one to describe the organic matter adsorption on PAC, yielding R^2 values above 0.995. In the Freundlich model, there exists a distribution of sites with different adsorption energies and more than one layer of adsorbates can adsorb onto the PAC. The value of n is between 1 and 5, indicating that all three activated carbons favorably adsorb organic matter from FPW. The value of $1/n$ for WP260 is the smallest, confirming that this material is the most adequate one among the three options. In addition, a value below unity implies chemisorption process (Foo and Hameed, 2010). Fig. 1C shows the results of adsorption equilibria tests at 293 K. The value of q_e decreased sharply at low PAC content and approached very small values close to zero for a dose larger than roughly 300 mg/L, even though not the entire amount of DOC was removed from the liquid phase (see Table 1). This result is indicative of the fact that the active sites of the adsorbents were not fully utilized and that the limiting factor was not the dose or the type of PAC, but possibly the nature of the DOC in the system, a fraction of which did not follow an equilibrium-driven partitioning with the adsorbent phase.

Among the various PACs, WP260 possessed the highest organics adsorption efficiency, consistent with adsorption isotherms. Therefore, WP260 was selected for the hybrid system with the most appropriate dose of 300 mg/L.

3.1.2 Adsorption kinetics

Fig. 1D shows the adsorption kinetics of DOC onto WP260. The adsorption was relatively fast within the first two hours, reaching a relative DOC value of 0.48, while it slowed down significantly after this time. The rapid initial adsorption regime may be attributed to the high concentration gradient between the adsorbate in solution and that on the solid phase, as well as to the high number of sites available for adsorption. Later during treatment, the adsorption becomes diffusion-controlled and other phenomena, such as the aggregation of DOC molecules, may reduce the kinetics of adsorption (Crittenden et al., 2012). Also, the affinity with PAC of DOC fractions may be lower for organic molecules that are still in suspension at later stages of the adsorption treatment. The experimental data were simulated using pseudo first-order and pseudo second-order models to examine the controlling mechanism of PAC adsorption, e.g., physical adsorption, mass transfer, and chemical reaction. As shown in Fig. S3 and Table S1 of the Supporting Information, the adsorption kinetics of DOC on WP260 may be simulated well by a pseudo-second-order kinetics model (correlation coefficients, $R^2 > 0.997$). The equilibrium concentration of DOC predicted by the pseudo second-order model agrees well with the experimental data, suggesting chemisorption as the rate-controlling step for the DOC adsorption onto WP260, consistent with what discussed above.

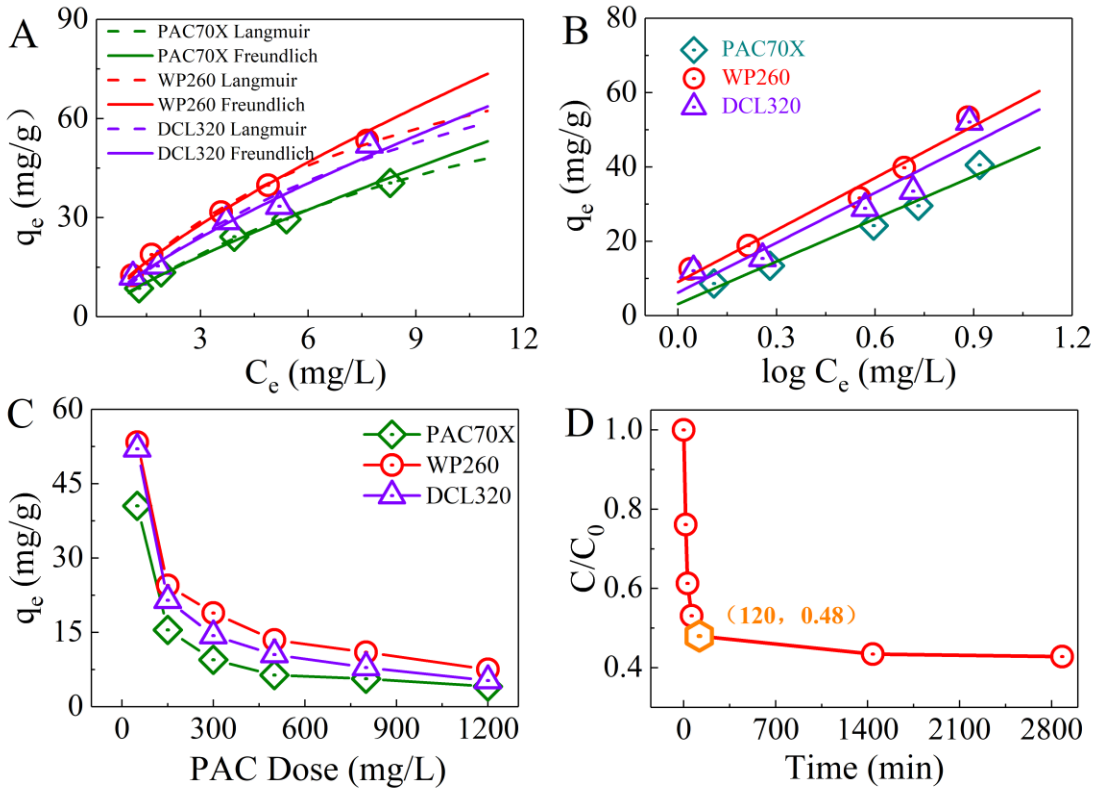

286

287 **Fig. 1**. Adsorption equilibria, kinetics, and models. (A) Adsorption isotherms of DOC adsorbing
288 from the coagulated FPW on different PACs (dose of 50 mg/L and total adsorption time of 48 h)
289 and best fittings with Freundlich and Langmuir models. (B) Adsorption isotherms of DOC
290 adsorbing from the coagulated FPW on different PACs (dose of 50 mg/L and total adsorption
291 time of 48 h) and best fittings with Temkin model. (C) Comparison of adsorption equilibria of
292 DOC from the coagulated FPW on different PACs for a total adsorption time of 48 h. (D)
293 Kinetics of adsorption of DOC from the coagulated FPW, with a dose of WP360 of 300 mg/L.
294 All the experiments were performed at pH 7.5 and at a temperature of 293 K.

295

296 **Table 3**. Isotherm fitting parameters for the adsorption of DOC from raw FPW onto WP260,
297 DCL320, and PAC70X powdered activated carbon

Specifications	Freundlich			Langmuir			Temkin		
	1/n	K_F	R^2	Q_M	K_L	R^2	B	K_T	R^2
WP260	0.73	12.43	0.995	109.89	0.12	0.981	46.66	1.57	0.977
PAC320	0.75	10.54	0.987	120.48	0.09	0.758	44.75	1.38	0.913
DCL70X	0.82	7.51	0.992	112.36	0.070	0.960	38.23	1.21	0.981

3.2 Effect of pretreatment on fouling in ultrafiltration

Various effluents were fed to the UF system to evaluate their fouling propensity, thus the efficacy of feed pre-treatment. In particular, different combinations of pre-treatment processes were assessed, including coagulation alone, PAC adsorption alone, and a sequence of the above, i.e., coagulation followed by adsorption. The transmembrane pressure of the UF system during the constant-flux treatment of FPW was monitored over time as an indication of membrane fouling and is shown in Figure 2A-C. The same initial flux of 50 L $m^{-2}h^{-1}$ was applied to all experiments. Obviously, as the operating time increased, TMP also increased because of fouling. The periodic hydraulic backwashing resulted in the discontinuous cycles shown in Figure 2. The TMP was maintained lower than 80 kPa, as above this value the UF performance can deteriorate (Jarzyńska and Pietruszka, 2011). As shown in Fig. 2A, the TMP increased significantly and rapidly while treating FPWs that had not undergone previous coagulation, suggesting that coagulation using aluminum coagulant can effectively reduce UF membrane fouling, which is in accordance with our previous research (Chang et al., 2019b). The growth rate of the measured TMP was also slowed down during the treatment of raw water filtered with a 0.45 μm pore-size filter (Fig. S4): the TFI was reduced by 49.4% compared to the TFI when the raw water was directly fed to the UF system. This result indicates that some large particulates and matter (>0.45

μm) can also increase the fouling of the UF membrane. Overall, the fouling rate decreased with the following order of feed water: raw FPW, FPW subject to adsorption only, FPW subject to microfiltration only, FPW subject to filtration and then adsorption, FPW subject to coagulation and then adsorption (Fig. 2D).

When the raw FPW was only pre-treated by PAC, the UF membrane fouling decreased with an increase in PAC dosage of 0-300 mg/L, as shown in Fig. 2B and E. Above the dosage of 300 mg/L, comparable UF fouling was observed up to 1,200 mg/L.. On the contrary, the opposite effect with PAC dose was observed for FPWs that were first treated by coagulation (Fig. 2C, F). There, fouling effects were significantly less critical than those observed for feed waters that were only treated by adsorption without prior coagulation. However, the TMP increased slightly with the increase in PAC dose. Indeed, as the PAC dose increased from 0 to 1200 mg/L, the TFI increased from 0.63 to 1.61 (Fig. 2F). This observation may be rationalized as PAC particles and gels accumulated on the surface to contribute in the formation of the fouling layer, as others have previously reported (Cheng-Fang Lin 1999; Zhang et al., 2003). Therefore, while the coagulation treatment helps remarkably in fouling reduction, the PAC should not be overdosed in the following adsorption step. Coagulation removed particles and colloids in suspension (Kong et al., 2017), preventing the formation of large settleable flocs with PAC. As such, PAC remained in suspension and could foul the UF membrane, actually representing the dominant factor in membrane fouling under these conditions.

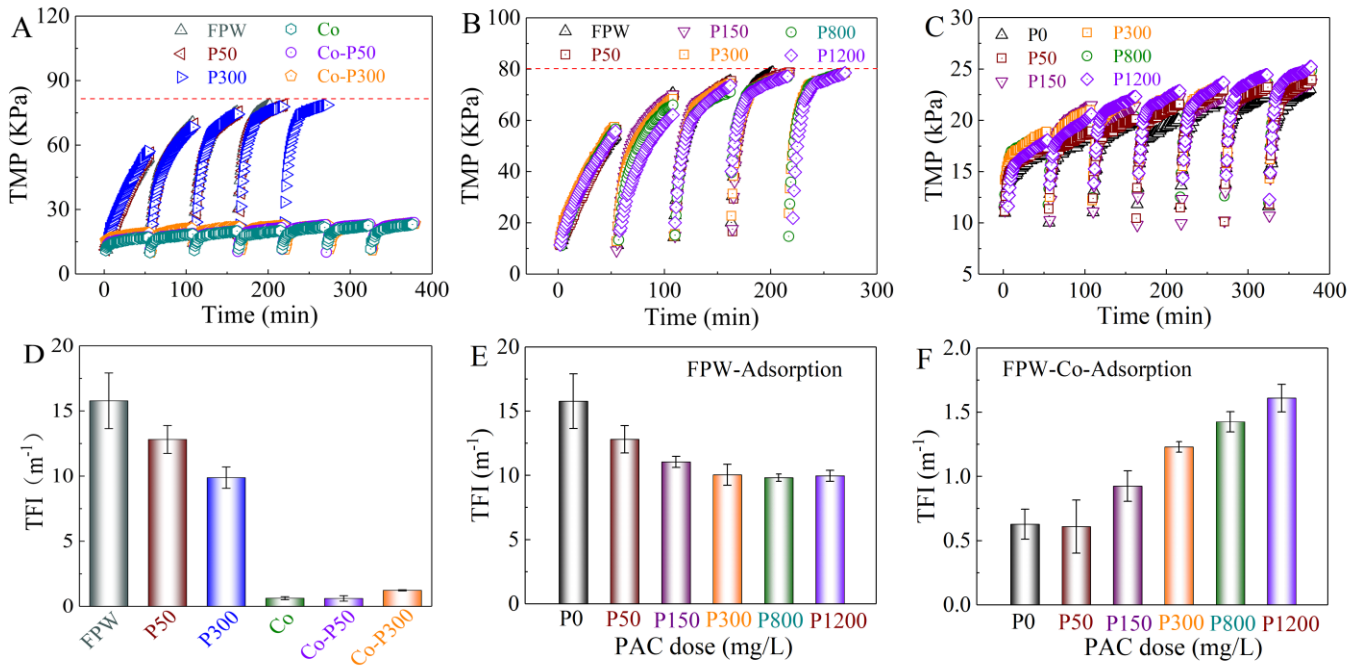

Fig. 2. UF membrane fouling expressed as transmembrane pressure (TMP) and total fouling index (TFI). (A, B, C) TMP as a function of time and (D, E, F) TFI when the UF system was applied to treat (A, D) effluents from different pre-treatment processes, (B, E) effluents treated by PAC adsorption without prior coagulation for different doses of WP260, and (C, F) effluents treated by coagulation followed by PAC adsorption for different doses of WP260. The labels indicate the following: "FPW" for raw influent water, "Co" for coagulation only, "P" for adsorption. The numbers in the labels refer to different PAC doses.

The FPW chemistry and fouling agents constantly change the membrane surface properties and membrane-foulant interactions during fouling (Bellona et al., 2004). To improve the understanding of UF performance with FPW, the fouled membranes and fouling layers were characterized. SEM-EDS analyses confirmed that the UF membrane surface was covered with a dense foulant layer following filtration of the raw FPW (Fig. 3A) or of FPW treated with

coagulation only (Fig. 3B). Specifically, the raw FPW created a thick and dense layer, consistent with the results presented by Chang et al.(Chang et al., 2019b) By contrast, when coagulated-adsorption water was treated in ultrafiltration (Fig. 3C, 3D), a thinner foulant layer covered the membrane surface and not its entirety was covered by foulants. Also, irregular particles appeared on the surface of the UF membrane when the adsorbent dose was 1200 mg/L compared to the adsorbent dose of 300 mg/L, suggesting the presence of PAC particles for high doses. This hypothesis is corroborated the relative content of carbon on the sample shown 4D (64.7%) was significantly higher than on that relative to 4C (49.1%). In general, the EDS analysis showed a large content of elements Cl, Na, C, and O, as well as high concentrations of Si, Ca, Mg, Al, S, Fe, Sr, and Ba on the fouled UF membrane surface, compared with the new PVDF membrane (Tab. S2). Although almost the same elements were detected on the surface of all the fouled membranes, the relative amounts of the various elements differed. The relative weight percentage of elements Mg, Ca, Fe, Ba decreased with the increase of WP260 dose, suggesting a larger removal for higher PAC concentrations during adsorption. Remarkably, almost no Ca, Ba, or Fe were detected on the surface of the UF membrane following treatment of water pretreated by both coagulation and adsorption (Fig. 3C, 3D). Comparing Fig. 2 and Fig. 3, the TFI values of the UF membrane were almost unchanged when fed with coagulation-adsorption treated water or only coagulation-treated water (Fig. 2), but the nature of the foulants on the surface of these membranes, provided by EDS analyses, is significantly different (Fig. 3). The results obtained in this study were similar to those found in the published literature (Chang et al., 2015; Remize et al., 2010). Although the total permeability could be almost completely restored, only part of the foulants were removed from the membrane, with a certain amount of foulants still deposited on the membrane surface.. In summary, the results presented in Fig. 3 and Fig. S5 of the Supporting

372 Information imply that coagulation combined with activated carbon adsorption has the potential
373 to greatly reduce fouling, in turn improving the membrane performance.

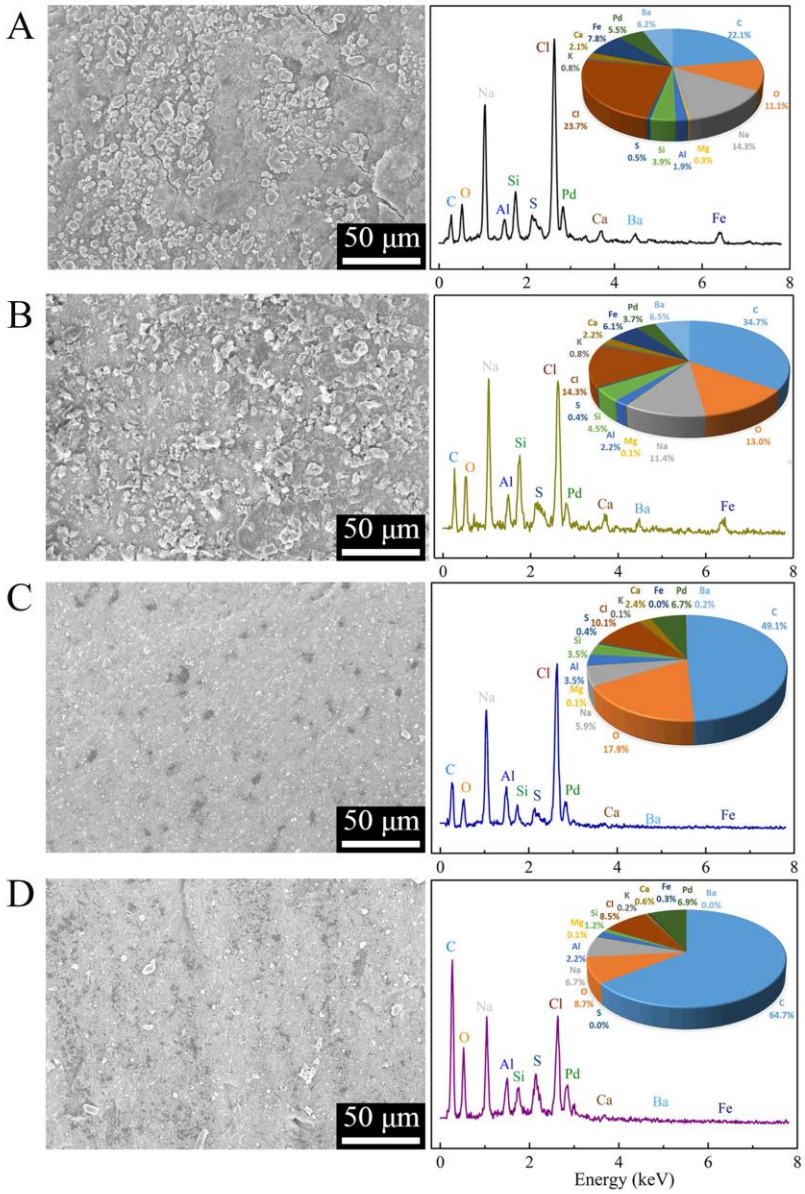

374

375 **Fig. 3**. SEM-EDS analyses of the UF membrane surface after fouling following the filtration of
376 effluents that had been treated with different pre-treatment processes. UF filtration of the (A) raw
377 FPW; (B) effluent from coagulation; (C) effluent from coagulation and adsorption at the WP260

dose of 300 mg/L, and (D) effluent from coagulation and adsorption at the WP260 dose of 1200 mg/L. All the experiments performed at constant flux of 50 LMH and temperature of 293 K.

3.3 Effect of pretreatment on fouling in reverse osmosis

The normalized water flux decline with different feed solutions of the RO process operating up to 50% recovery is presented in Fig. 4. The permeate flux decreased with increasing recovery, which is mainly due to the increase in the osmotic pressure of the retentate. In general, the measured flux across the membrane was higher for larger PAC doses applied in the adsorption pre-treatment. This effect was observed up to a PAC dose of 300 mg/L, above which the RO flux was not function of the adsorption conditions. Specifically, adsorption pre-treatment performed with 300 mg/L of WP260 reduced the fouling in RO and increased flux by 10.8%. This was mainly due to the difference in the influent water quality of the RO. In terms of organic matter (DOC, UV_{254}) and turbidity, PAC at a dosage of 300 mg/L could ensure that the influent water quality of the RO had basically the lowest concentration of pollutants, as discussed in detail in Section 3.4. In addition, the positive effect of adsorption is expected to be even more pronounced for longer operating time and if cross-flow filtration is used instead of dead-end mode (Quay et al., 2018).

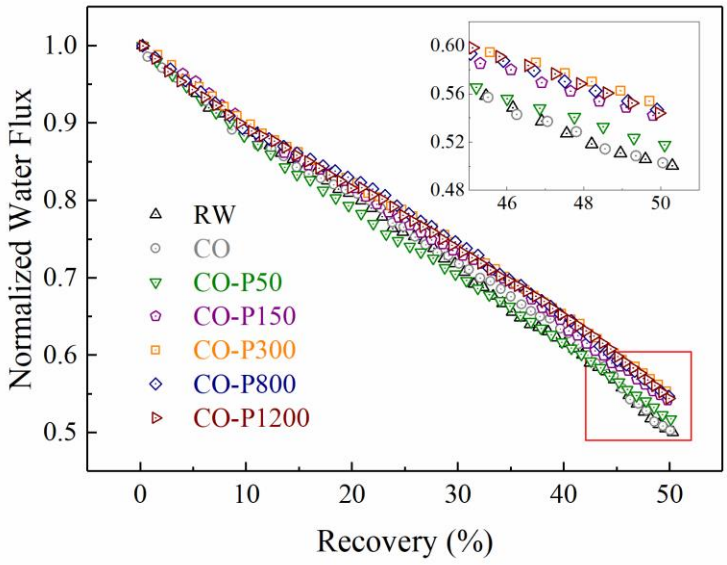

Fig. 4. Normalized water flux during RO desalination as a function of recovery for feed water following UF treatment and that that had been subject to different pre-treatment processes. The applied pressure was 5.5 MPa and the temperature during RO filtration was 293 K.

The surface morphology and elemental composition of the fouling layer was analyzed on RO membranes following the treatment of effluents from the UF step that were subject to different pre-treatments. The results from SEM-EDS analyses are shown in Fig. 5. C, O, and S are the main elements observed on the surface of the RO membranes, similarly to the pristine membrane (Tab.S2). Nevertheless, numerous particles of mostly $CaCO_3$ and to a less extent of $BaCO_3$ were visible on the membrane fed with the raw FPW only treated by UF (Fig. 5A), as also shown in a previous report (Guo et al., 2018). The presence and the size of these crystals was significantly reduced when the water was pre-treated by coagulation (Fig. 5B). This effect is caused by coagulation, which reduced the pH and slowed down the precipitation of calcium carbonate. When PAC adsorption was applied, either at a concentration of activated carbon of 300 mg/L or

1200 mg/L, only trace amounts of Ca and Ba were present on the surface of the membrane. In this case, the pH, alkalinity and Ca^{2+} concentration were all key factors affecting the $CaCO_3$ scaling of the RO membrane (Table S3). These observations confirm the effectiveness of coagulation and PAC adsorption also to reduce scaling in the final RO step.

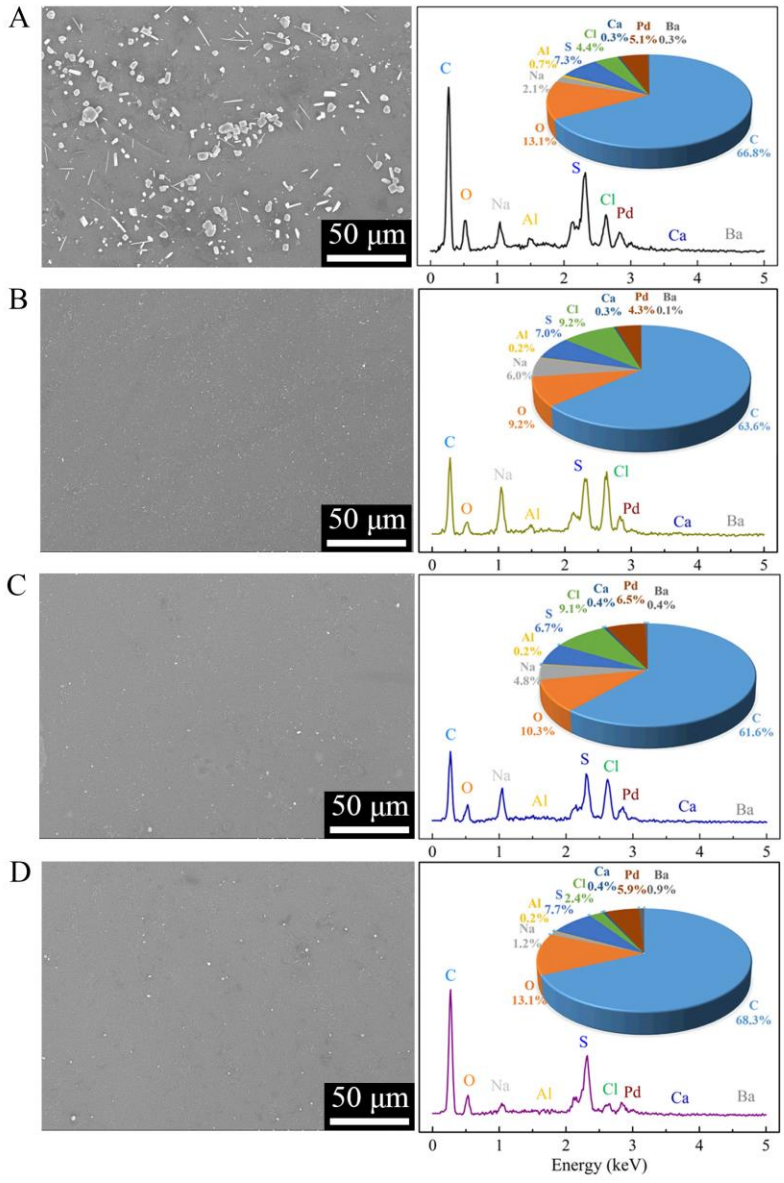

Fig. 5. SEM-EDS analyses of the RO membrane surface after fouling following the desalination of UF effluents that had been treated with different pre-treatment processes. RO desalination of

416 the UF permeate from the treatment of the (A) raw FPW; (B) effluent from coagulation; (C)
417 effluent from coagulation and adsorption at the WP260 dose of 300 mg/L, and (D) effluent from
418 coagulation and adsorption at the WP260 dose of 1200 mg/L. All the experiments performed at
419 an applied pressure of 55 bar, final recovery of 50%, and temperature of 293 K.

420

421 **3.4 Quality of the effluents and of the final water stream**

422 Fig. 6 summarizes the removal rates of different classes of contaminants exiting the adsorption
423 step, the ultrafiltration step, and the reverse osmosis steps, when the treatment units were
424 challenged by waters pretreated by different processes. Coagulation reduced the DOC by 64.2%,
425 and the addition of 300 mg/L PAC further reduced this parameter by 48.5%. In addition,
426 coagulation had a good removal effect (91.6%) on turbidity. Adsorption following coagulation
427 could further remove turbidity and reduce the turbidity of the effluent to a value below 10 NTU.
428 The removal of DOC, UV_{254}, and turbidity typically increased at higher dosages of PAC.
429 However, very similar removals were observed for PAC amounts of 300 mg/L and 1200 mg/L,
430 suggesting that 300 mg/L was the optimal dose for PAC adsorption of FPW, a result that is in
431 complete accordance with the results of membrane fouling. The same organic removal rate
432 previously observed by James et al. was achieved in this study but with roughly half the dose of
433 PAC (Rosenblum et al., 2016). It should be noted that when the raw FPW was directly fed to the
434 UF step, both the DOC and the UV_{254} were significantly reduced in this step, possibly because
435 the large particulates adhered to some organic matter, thus helping in its removal. However,
436 feeding the UF directly with non-pretreated FPW is not a viable option, as discussed above and
437 based on fouling results. As expected, UF abated the turbidity while it had negligible removal of
438 ions. Finally, RO removed TDS very efficiently. Overall, the best system combining all the

treatment steps, i.e., coagulation followed by adsorption with 300 mg/L of PAC followed by UF and RO, achieved a total ion reduction of more than 98.6%, and a DOC removal rate of 95.5%. The quality of this effluent, also summarized in the rightmost column of Table 1, reached the strict reuse standards for beneficial drilling applications and irrigation (Alzahrani and Mohammad, 2014). In addition, the cost data for each process unit (Table S4) are presented in the SI based on the relevant literature. The cost of the coagulation-adsorption-UF-RO process is lower than other FPW treatment schemes including, for example, FO or mechanical vapor compression. Therefore, the scheme proposed here has potential for the treatment of shale gas FPW in China in the future.

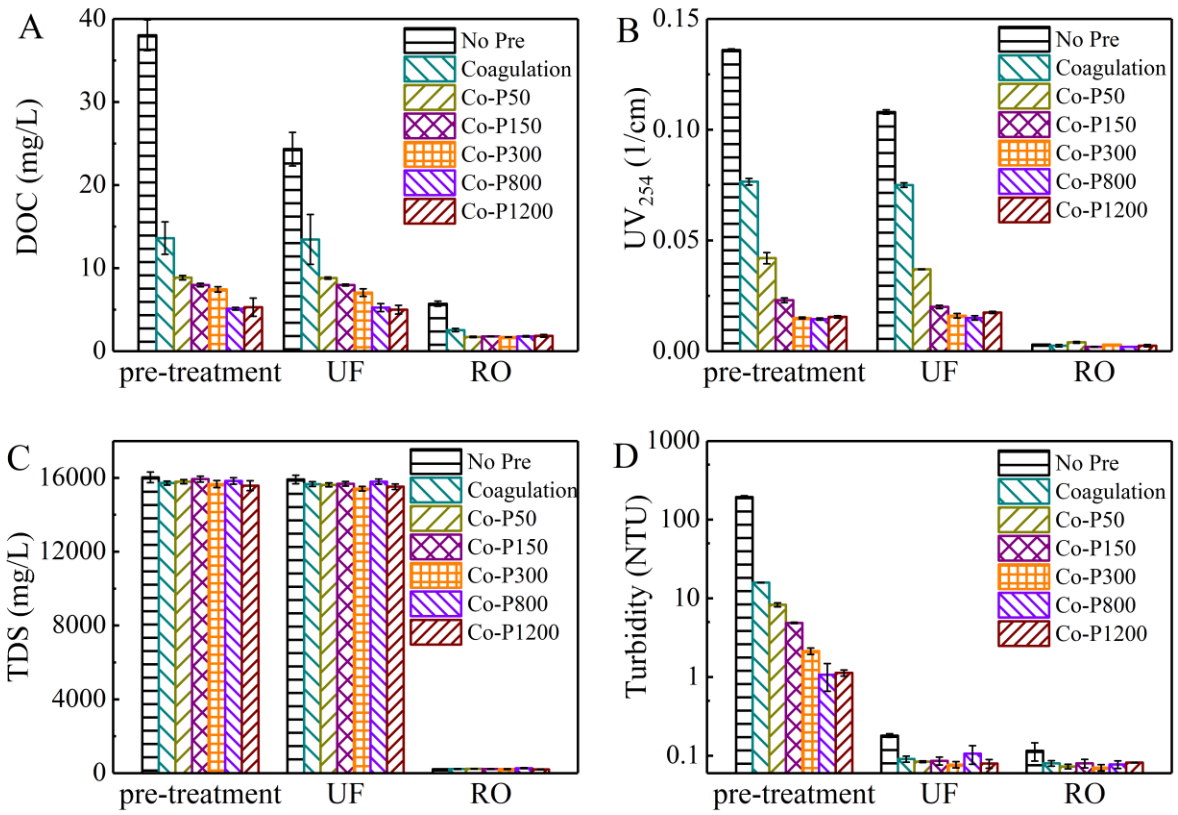

Fig. 6. Contents of different contaminants, specifically, (A) DOC; (B) UV_{254}; (C) TDS; and (D)

turbidity obtained at different stages of the treatment systems and for effluents that were pre-treated by different processes. The label "No Pre" indicates raw water without any pre-treatment.

3.5 Ion removal during activated carbon adsorption

Although coagulation, adsorption, and UF did not remove TDS at a significant rate, it is of further interest to evaluate the ability of pre-treatments to remove some specific ions from FPW. The effect of coagulation and UF on specific ion removal was previously studied (Chang et al., 2019b; Guo et al., 2018). Here, we focus on the removal rates of different ions from the coagulated FPW by adsorption, presented in Figure 7. The results indicate a competition effect for the adsorption of cations, whereby the removal rate may be ranked in the folloing ascending order: Na^+ (2.4%) < NH_4^+ (16.8%) < Ca^{2+} (22.0%) < Mg^{2+} (23.9%) < K^+ (28.6%) < Ba^{2+} (29.2%) < Sr^{2+} (49.5%) < DOC (61.7%). The removal rate of anions may be instead arranged in the order: Cl^- (1.3%) < Br^- (4.7%) < NO_3^- (7.9%) < NO_2^- (8.1%) < F^- (18.3%) < DOC (61.7%). Clearly, the removal of divalent ions was greater than that of monovalent ions, as the adsorption of negatively charge DOC promotes the concurrent removal of cations associated with the organic molecules electrostatically or by complexation (Foo and Hameed, 2010; Gao et al., 2018). Interestingly, the removal of K^+ was higher than for other divalent cations known to interact favorably with organic matter, such as calcium. This result may be partially rationalized with the overall larger size of K^+, which are thus associated with a more favorable energy of adsorption (Neugebauer and Scheffler, 1992). Finally, the kinetics of removal of the various ions by adsorption are presented in Fig. S6.

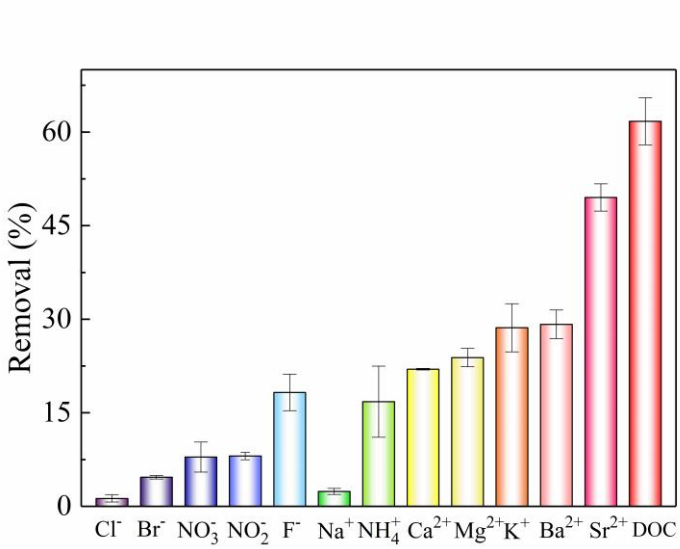

Fig 7. Removal rates of DOC, anions, and cations during the adsorption step with WP260 powdered activated carbon at the dose of 300 mg/L. The adsorbate was coagulated FPW.

4. Conclusions

Shale gas flowback and produced water, as a complex mixture of fracturing fluid and formation water, may be effectively reused if appropriately treated. This study provides a new FPW treatment train consisting of coagulation, adsorption followed by UF and RO desalination. In particular, this work focused on the mechanism of adsorption and on the effects of pre-treatment on effluent quality and membrane fouling control. The following main conclusions can be drawn from the results:

1. The overall system performed a reliable treatment of the specific FPW to obtain a high-quality product water with characteristics compatible with its reuse. Therefore, this study provides a potential reference for a centralized shale gas FPW treatment plant in the Sichuan Basin of China.

2. Coagulation and adsorption are valid pre-treatment for membrane processes. Interesting patterns were observed: when PAC was directly applied to adsorb contaminants from the raw FPW, the UF membrane fouling decreased with increasing PAC dosage. However, when coagulation was added before adsorption, UF membrane fouling increased with increasing PAC dosage. However, in this latter case, membrane fouling was much smaller than when UF was applied to an effluent pre-treated only by adsorption. Therefore, adsorption should be preceded by coagulation for improved performance of the system.

3. There was an optimal activated carbon dosage of 300 mg/L for the adsorption treatment. This dose resulted in the greatest gain in terms of fouling reduction in both UF and RO and in terms of quality of the final product water.

4. During the adsorption process, ions were removed at different rates, also due to co-sorption of cations with the organic matter. The mechanism of the adsorption of ions by PAC in FPW needs further research.

Appendix A. Supplementary material

The supporting information is available free of charge.

The size distributions of three adsorbents; linear plots of pseudo first order and pseudo second order adsorption kinetics of DOC on WP260; summary of adsorption kinetic parameters; EDS analyses of the new UF and RO membranes surface.

Acknowledgments

This work was supported by the National Natural Science Foundation of China (51678377, 51708371), the Applied Basic Research of Sichuan Province (2017JY0238), the Key Projects in

the Science & Technology Program of Sichuan Province (2018SZDZX0027), and China Postdoctoral Science Foundation (2018T110973, 2017M612965). Alberto Tiraferri acknowledges the support of Compagnia di San Paolo and Politecnico di Torino through the project FLOWING. The views and ideas expressed herein are solely those of the authors and do not represent the ideas of the funding agencies in any form.

References

Alzahrani S, Mohammad AW. Challenges and trends in membrane technology implementation for produced water treatment: A review. Journal of Water Process Engineering 2014; 4: 107-133.

Amin Reyhania KS, Seyed Mahdi Seyed Shahabadia,Fatemeh Rekabdarc, Ali Gheshlaghi. Optimization of operating conditions in ultrafiltration process for produced water treatment via Taguchi methodology. Desalination and Water Treatment 2015; 54: 2669-2680.

Angin D. Utilization of activated carbon produced from fruit juice industry solid waste for the adsorption of Yellow 18 from aqueous solutions. Bioresource technology 2014; 168: 259-266.

Annevelink MP, Meesters JA, Hendriks AJ. Environmental contamination due to shale gas development. Science of the Total Environment 2016; 550: 431-438.

Barbot E, Vidic NS, Gregory KB, Vidic RD. Spatial and temporal correlation of water quality parameters of produced waters from Devonian-Age shale following hydraulic fracturing. Environmental Science & Technology 2013; 47: 2562-2569.

Bellona C, Drewes JE, Xu P, Amy G. Factors affecting the rejection of organic solutes during NF/RO treatment--a literature review. Water research 2004; 38: 2795-2809.

Butkovskyi A, Bruning H, Kools SAE, Rijnaarts HHM, Van Wezel AP. Organic Pollutants in Shale Gas Flowback and Produced Waters: Identification, Potential Ecological Impact, and Implications for Treatment Strategies. Environmental Science & Technology 2017; 51: 4740-4754.

Chang H, Li T, Liu B, Vidic RD, Elimelech M, Crittenden JC. Potential and implemented membrane-based technologies for the treatment and reuse of flowback and produced water from shale gas and oil plays: A review. Desalination 2019a; 455: 34-57.

Chang H, Liang H, Qu F, Shao S, Yu H, Liu B, et al. Role of backwash water composition in alleviating ultrafiltration membrane fouling by sodium alginate and the effectiveness of salt backwashing. Journal of Membrane Science 2016; 499: 429-441.

Chang H, Liu B, Yang B, Yang X, Guo C, He Q, et al. An integrated coagulation-ultrafiltration-nanofiltration process for internal reuse of shale gas flowback and produced water. Separation and Purification Technology 2019b; 211: 310-321.

Chang H, Liu T, He Q, Li D, Crittenden J, Liu B. Removal of calcium and magnesium ions from shale gas flowback water by chemically activated zeolite. Water Science & Technology 2017; 76: 575-583.

Chang H, Qu F, Liu B, Yu H, Li K, Shao S, et al. Hydraulic irreversibility of ultrafiltration membrane fouling by humic acid: Effects of membrane properties and backwash water composition. Journal of Membrane Science 2015; 493: 723-733.

Chen G, Wang Z, Nghiem LD, Li X-M, Xie M, Zhao B, et al. Treatment of shale gas drilling flowback fluids (SGDFs) by forward osmosis: Membrane fouling and mitigation. Desalination 2015; 366: 113-120.

Cheng-Fang Lin Y-JH, Oliver J Hao Ultrafiltration processes for removing humic substances: effect of molecular weight fractions and PAC treatment. Water Research 1999; 33: 1252-1264.

Cheng W, Ding C, Sun Y, Wang X. Fabrication of fungus/attapulgite composites and their

557 removal of U(VI) from aqueous solution. Chemical Engineering Journal 2015; 269: 1-8.
558 Crittenden JC, Trussell RR, Hand DW. MWH's water treatment: principles and design (third
559 edition), 2012.
560 Elimelech M, Phillip WA. The future of seawater desalination: energy, technology, and the
561 environment. Science 2011; 333: 712-717.
562 Estrada JM, Bhamidimarri R. A review of the issues and treatment options for wastewater from
563 shale gas extraction by hydraulic fracturing. Fuel 2016; 182: 292-303.
564 Foo KY, Hameed BH. Insights into the modeling of adsorption isotherm systems. Chemical
565 Engineering Journal 2010; 156: 2-10.
566 Gao H, Cao R, Xu X, Xue J, Zhang S, Hayat T, et al. Surface Area- and Structure-Dependent
567 Effects of LDH for Highly Efficient Dye Removal. ACS Sustainable Chemistry &
568 Engineering 2018; 7: 905-915.
569 Guo C, Chang H, Liu B, He Q, Xiong B, Kumar M, et al. A combined ultrafiltration–reverse
570 osmosis process for external reuse of Weiyuan shale gas flowback and produced water.
571 Environmental Science: Water Research & Technology 2018; 4: 942-955.
572 Harkness JS, Dwyer GS, Warner NR, Parker KM, Mitch WA, Vengosh A. Iodide, bromide, and
573 ammonium in hydraulic fracturing and oil and gas wastewaters: environmental
574 implications. Environmental Science & Technology 2015; 49: 1955-1963.
575 Howarth RW, Ingraffea A, Engelder T. Natural gas: Should fracking stop? Nature 2011; 477:
576 271-275.
577 Huang L, Fan H, Xie H, Huang Z. Experimental study of treatment processes for shale gas
578 fracturing flowback fluid in the eastern Sichuan Basin. Desalination and Water Treatment
579 2016; 57: 24299-24312.
580 Jarzyńska M, Pietruszka M. The application of the Kedem–Katchalsky equations to membrane
581 transport of ethyl alcohol and glucose. Desalination 2011; 280: 14-19.
582 Kondash A, Vengosh A. Water footprint of hydraulic fracturing. Environmental Science &
583 Technology Letters 2015; 2: 276-280.
584 Kong F-x, Chen J-f, Wang H-m, Liu X-n, Wang X-m, Wen X, et al. Application of coagulation-
585 UF hybrid process for shale gas fracturing flowback water recycling: Performance and
586 fouling analysis. Journal of Membrane Science 2017; 524: 460-469.
587 Liu Q-S, Wang P, Zhao S-S, Zhang W. Treatment of an industrial chemical waste-water using a
588 granular activated carbon adsorption-microwave regeneration process. Journal of
589 Chemical Technology & Biotechnology 2012; 87: 1004-1009.
590 Luek JL, Gonsior M. Organic compounds in hydraulic fracturing fluids and wastewaters: A
591 review. Water Research 2017; 123: 536-548.
592 Manz KE, Haerr G, Lucchesi J, Carter KE. Adsorption of hydraulic fracturing fluid components
593 2-butoxyethanol and furfural onto granular activated carbon and shale rock.
594 Chemosphere 2016; 164: 585-592.
595 Neugebauer J, Scheffler M. Adsorbate-substrate and adsorbate-adsorbate interactions of Na and
596 K adlayers on Al(111). Physical Review B 1992; 46: 16067-16080.
597 Nguyen AH, Tobiason JE, Howe KJ. Fouling indices for low pressure hollow fiber membrane
598 performance assessment. Water Research 2011; 45: 2627-2637.
599 Quay AN, Tong T, Hashmi SM, Zhou Y, Zhao S, Elimelech M. Combined Organic Fouling and
600 Inorganic Scaling in Reverse Osmosis: Role of Protein-Silica Interactions. Environmental
601 Science & Technology 2018; 52: 9145-9153.
602 Remize PJ, Guigui C, Cabassud C. Evaluation of backwash efficiency, definition of remaining

603 fouling and characterisation of its contribution in irreversible fouling: Case of drinking
604 water production by air-assisted ultra-filtration. Journal of Membrane Science 2010; 355:
605 104-111.
606 Rosenblum JS, Sitterley KA, Thurman EM, Ferrer I, Linden KG. Hydraulic fracturing
607 wastewater treatment by coagulation-adsorption for removal of organic compounds and
608 turbidity. Journal of Environmental Chemical Engineering 2016; 4: 1978-1984.
609 Shaffer DL, Arias Chavez LH, Ben-Sasson M, Romero-Vargas Castrillon S, Yip NY, Elimelech
610 M. Desalination and reuse of high-salinity shale gas produced water: drivers,
611 technologies, and future directions. Environmental Science & Technology 2013; 47:
612 9569-9583.
613 Shao S, Cai L, Li K, Li J, Du X, Li G, et al. Deposition of powdered activated carbon (PAC) on
614 ultrafiltration (UF) membrane surface: influencing factors and mechanisms. Journal of
615 Membrane Science 2017; 530: 104-111.
616 Sontheimer H, Crittenden JC, Summers RS. Activated carbon for water treatment. Vol 2.
617 American Water Works Association 1988.
618 Stoll ZA, Forrestal C, Ren ZJ, Xu P. Shale gas produced water treatment using innovative
619 microbial capacitive desalination cell. Journal of Hazardous Materials 2015; 283: 847-
620 855.
621 Vengosh A, Jackson RB, Warner N, Darrah TH, Kondash A. A critical review of the risks to
622 water resources from unconventional shale gas development and hydraulic fracturing in
623 the United States. Environmental Science & Technology 2014; 48: 8334-8348.
624 Vidic RD, Brantley SL, Vandenbossche JM, Yoxtheimer D, Abad JD. Impact of shale gas
625 development on regional water quality. Science 2013; 340: 1235009.
626 Wang H, Qu F, Ding A, Liang H, Jia R, Li K, et al. Combined effects of PAC adsorption and in
627 situ chlorination on membrane fouling in a pilot-scale coagulation and ultrafiltration
628 process. Chemical Engineering Journal 2016; 283: 1374-1383.
629 Xiong B, Zydney AL, Kumar M. Fouling of microfiltration membranes by flowback and
630 produced waters from the Marcellus shale gas play. Water Research 2016; 99: 162-170.
631 Zhang MM, Li C, Benjamin MM, Chang YJ. Fouling and natural organic matter removal in
632 adsorben/membrane systems for drinking water treatment. Environmental Science &
633 Technology 2003 37: 1663-1669.
634 Zhang Z, Zhuang Y, Li J, Zhou Z, Chen S. Feasibility evaluation of the treatment and recycling
635 of shale gas produced water: a case study of the first shale gas field in the Eastern
636 Sichuan Basin, China. Environmental Science: Water Research & Technology 2019; 5:
637 358-369.
638 Zou C, Ni Y, Li J, Kondash A, Coyte R, Lauer N, et al. The water footprint of hydraulic
639 fracturing in Sichuan Basin, China. Science of the Total Environment 2018; 630: 349-356.
640